Inorganic Chemistry

Article

pubs.acs.org/IC

Noncovalent Interactions in Peri-Substituted Chalconium Acenaphthene and Naphthalene Salts: A Combined Experimental, Crystallographic, Computational, and Solid-State NMR Study

Fergus R. Knight,* Rebecca A. M. Randall, Kasun S. Athukorala Arachchige, Lucy Wakefield, John M. Griffin, Sharon E. Ashbrook, Michael Bühl, Alexandra M. Z. Slawin, and J. Derek Woollins

EaStCHEM, School of Chemistry, University of St. Andrews, St. Andrews, Fife, KY16 9ST, United Kingdom

Supporting Information

ABSTRACT: Twelve related monocation chalconium salts [{Nap(EPh)(E′Ph)Me}$^+${CF_3SO_3}$^-$] **2**−**4**, [{Acenap(Br)(EPh)Me}{CF_3SO_3}$^-$] **5**−**7**, and [{Acenap(EPh)(E′Ph)Me}$^+${CF_3SO_3}$^-$] **8**−**13** have been prepared and structurally characterized. For their synthesis naphthalene compounds [Nap(EPh)(E′Ph)] (Nap = naphthalene-1,8-diyl; E/E′ = S, Se, Te) **N2**−**N4** and associated acenaphthene derivatives [Acenap(X)(EPh)]/[Acenap(EPh)(E′Ph)] (Acenap = acenaphthene-5,6-diyl; E/E′ = S, Se, Te; X = Br) **A5**−**A13** were independently treated with a single molar equivalent of methyl trifluoromethanesulfonate (MeOTf). In addition, reaction of bis-tellurium compound **A10** with 2 equiv of MeOTf afforded the doubly methylated dication salt [{Acenap(TePhMe)$_2$}$^{2+}${$(CF_3SO_3)_2$}$^{2-}$}] **14**. The distortion of the rigid naphthalene and acenaphthene backbone away from ideal was investigated in each case and correlated in general with the steric bulk of the interacting atoms located at the proximal peri positions. Naturally, introduction of the ethane linker in acenaphthene compounds increased the splay of the bay region compared with equivalent naphthalene derivatives resulting in greater peri distances. The conformation of the aromatic rings and subsequent location of p-type lone pairs has a significant impact on the geometry of the peri region, with anomalies in peri separations correlated to the ability of the frontier orbitals to take part in attractive or repulsive interactions. In all but one of the monocations a quasi-linear three-body C_{Me}−E···Z (E = Te, Se, S; Z = Br/E) fragment provides an attractive component for the E···Z interaction. Density functional studies confirmed these interactions and suggested the onset of formation of three-center, four-electron bonding under appropriate geometric conditions, becoming more prevalent as heavier congeners are introduced along the series. The increasingly large *J* values for Se−Se, Te−Se, and Te−Te coupling observed in the ^{77}Se and ^{125}Te NMR spectra for **1**, **3**, **4**, **9**, **10**, and **13** give further evidence for the existence of a weakly attractive through-space interaction.

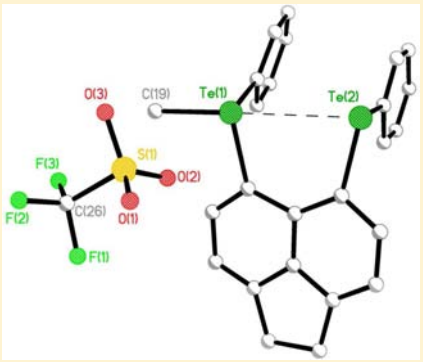

INTRODUCTION

Pioneering work on the electronic theory of the covalent bond led to a greater understanding of strong bonding (covalent/ionic),[1] but ambiguity over the role of weak inter- and intramolecular noncovalent interactions continues to intrigue chemists.[2−9] Designing structural architectures which invoke novel and unusual bonding interactions is indispensable for developing the theory of nonbonded forces and the chemical bond and is therefore an intriguing field of study.[10,11]

In this context, we previously utilized the unique geometric constraints associated with peri substitution and the rigidity of the naphthalene[12] and acenaphthene[13] backbones to investigate noncovalent forces occurring in mixed-donor ligands. Our early work focused on naphthalene, synthesizing dichalcogenide ligands,[14] unusual phosphorus compounds,[15] and mixed-donor phosphorus−chalcogen systems.[16] More recently, we prepared a series of 1,8-disubstituted naphthalene derivatives that contain chalcogen or halogen moieties at the peri positions [{Nap(EPh)(E′Ph)}/{Nap(X)(EPh)} (X = Br, I; E = S, Se, Te)][17−20] and an analogous series employing the alternative acenaphthene scaffold [{Acenap(X)(EPh)}/{Acenap(EPh)(E′Ph)} (X = Br, I; E = S, Se, Te)].[21,22] These systems constrain the bulky halogen and chalcogen congeners in sterically demanding position, at distances closer than the sum of their respective van der Waals radii, inducing direct overlap of orbitals, leading to the onset of weakly bonding 3c-4e-type interactions under appropriate geometric conditions.[11,17,19,21]

Evidence supporting weak noncovalent peri interactions in these compounds is observed in the respective ^{77}Se and ^{125}Te NMR spectra.[17,21] Furukawa et al. identified a similar interaction between telluronio−tellurenyl groups at the peri positions of telluronium salt **1** (Figure 1) formed following treatment of 1,8-bis(phenyltelluro)naphthalene [Nap(TePh)$_2$] **N1** (Figure 1) with methyl trifluoromethanesulfonate (MeOTf).[23] The ^{125}Te NMR spectrum of **1** showed two peaks at δ = 656 (Te$^+$) and 557 ppm (Te), each peak exhibiting

Received: July 25, 2012
Published: September 24, 2012

   dx.doi.org/10.1021/ic301627y | *Inorg. Chem.* 2012, 51, 11087−11097

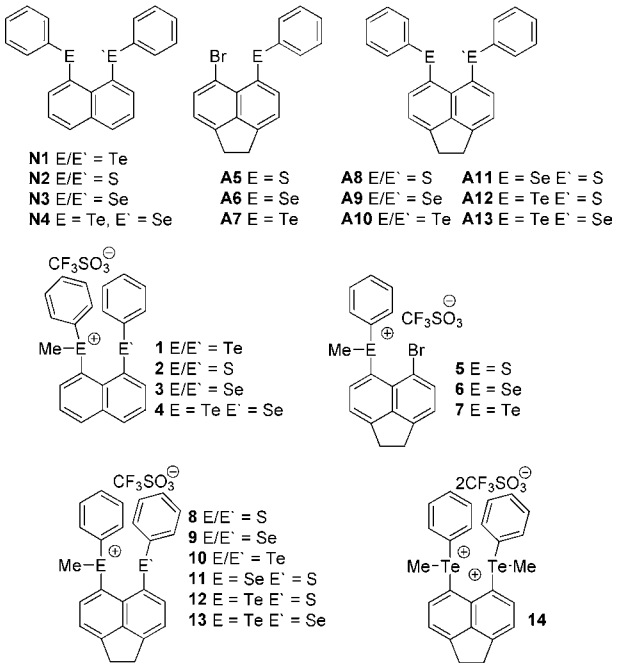

Figure 1. Monocation (**1**–**13**) and dication (**14**) chalconium salts formed from the reaction of naphthalene **N1**–**N4** and acenaphthene **A5**–**A13** derivatives with methyl trifluoromethanesulfonate (methyl triflate).

satellites due to ^{125}Te–^{125}Te coupling with the large coupling constants of J_{TeTe} = 1093 Hz attributed to a peri interaction.[23]

The work presented here complements our earlier studies of noncovalent interactions in naphthalene and acenaphthene chalcogenides[17,19,21] and the work initially undertaken by Furukawa et al. on tellurium–tellurium peri interactions in 1,8-ditelluronaphthalenes.[23] Herein we report a complete synthetic and structural study of associated monocation chalconium salts **2**–**13** and dication **14** formed from reaction of naphthalenes **N2**–**N4**[17] and acenaphthenes **A5**–**A13**[21] with MeOTf and an investigation of the potential nonbonding interactions associated with these types of systems (Figure 1).

RESULTS AND DISCUSSION

Synthesis of Chalconium Salts 2–14. Naphthalene compounds [Nap(EPh)(E′Ph)] (Nap = naphthalene-1,8-diyl; E/E′ = S, Se, Te) **N2**–**N4**[17] (Figure 1) and associated acenaphthene derivatives [Acenap(Z)(EPh)] (Acenap = acenaphthene-5,6-diyl; Z = Br, SPh, SePh, TePh; E = S, Se, Te) **A5**–**A13**[21] (Figure 1) were independently treated with methyl trifluoromethanesulfonate (MeOTf). For the synthesis of monocation chalconium salts **2**–**13** (Figure 1), methylation reactions were carried out using a 1:1 molar ratio of MeOTf to chalcogen derivative and run in dichloromethane under an oxygen- and a moisture-free nitrogen atmosphere (yield 87–96%). Under identical reaction conditions, treatment of 5,6-bis(phenyltelluro)acenaphthene **A10**[21] with 2 mol equiv of MeOTf afforded the dication chalconium salt **14** (yield 54%). Corresponding reactions of the remaining group of chalcogen derivatives with a similar loading of methyl triflate exclusively afforded the monocation chalconium salt in each case. All compounds obtained (**2**–**14**) were characterized by multinuclear magnetic resonance and IR spectroscopies and mass spectrometry, and the homogeneity of the new compounds was where possible confirmed by microanalysis. Solid-state and solution ^{77}Se and ^{125}Te NMR spectroscopic data can be found in Table 1 (and Table S1, Supporting Information).

The respective acenaphthene NMR signals for compounds **9**, **10**, and **13** display an upfield shift, lying at lower chemical shifts, indicating the nuclei are more shielded than in equivalent naphthalene salts **3**, **1**, and **4**, respectively. The ^{125}Te NMR spectrum of **10** is comparable with the data reported for the naphthalene telluronium salt **1** by Furukawa et al.:[23] two peaks at δ = 641 (Te$^+$) and 522 ppm (Te), each peak exhibiting satellites due to ^{125}Te–^{125}Te coupling. Indication of a strong through-space peri interaction is observed between the telluronio and the tellurenyl groups, with large coupling constants (J_{TeTe} = 946 Hz) of a similar magnitude to the reported naphthalene derivative (**1** J_{TeTe} = 1093 Hz[23]).

Solution and Solid-State NMR Studies. In contrast, the significantly smaller J values observed for ^{77}Se–^{77}Se coupling [**3** (167 Hz); **9** (141 Hz)] in the ^{77}Se NMR spectra for analogous selenonium salts **3** [δ = 436 (Se$^+$), 392 ppm (Se)] and **9** [δ = 422 (Se$^+$), 366 ppm (Se)] implies a weaker through-space interaction is occurring in each case. A more direct comparison is possible through the corresponding reduced coupling constants K, which decrease by ca. 60% on going from **1** (K = 9.0.1021 kg m^{-2} s^{-2} A^{-2}) to **3** (K = 3.8.1021 kg m^{-2} s^{-2} A^{-2}). As might be expected, the mixed-telluronio–selanyl compounds **4** and **13** display properties in between those of the bis-tellurium and bis-selenium analogues. The reciprocal ^{125}Te NMR and ^{77}Se NMR spectra for both compounds exhibit single peaks [**4** δ_{Te} = 706 ppm, δ_{Se} = 347 ppm; **13** δ_{Te} = 679 ppm, δ_{Se} = 322 ppm] with satellites attributed to ^{125}Te–^{77}Se coupling. The relatively large J values [**4** (429 Hz); **13** (382 Hz)], lying between those of the telluronium salts (**1**, **10**) and selenonium salts (**3**, **9**), indicate a potential weakly attractive through-space interaction.

Table 1. ^{77}Se and ^{125}Te NMR Spectroscopy Data[a]

	N3[23]	3	A6[21]	6	A9[21]	9	A11[21]	11	N4[17]	4	A13[21]	13
peri atoms	Se, Se	Se$^+$, Se	Se, Br	Se$^+$, Br	Se, Se	Se$^+$, Se	Se, S	Se$^+$, S	Te, Se	Te$^+$, Se	Te, Se	Te$^+$, Se
^{77}Se solution NMR	429	436, 392	424	420	408	422, 366	434	431	363	347	341	323
^{77}Se solid-state NMR					426, 400	427, 375	433	442			350	336, 319
J (solution NMR)		167				141				429		382
	N1[17]	**1**[23]	**A7**[21]	**7**	**A10**[21]	**10**	**A12**[21]	**12**	**14**			
peri atoms	Te, Te	Te$^+$, Te	Te, Br	Te$^+$, Br	Te, Te	Te$^+$, Te	Te, S	Te$^+$, S	Te$^+$, Te$^+$			
^{125}Te solution NMR	620	656, 557	696	693	586	641, 522	689	694	677	688 706	663	679
J (^{125}Te solution NMR)		1093				946				−834 429	−716	382
^{125}Te solid-state NMR					595, 523	665, 551	705	695			684	706, 682

[a]Solution spectra of parent compounds **3** and **4** were run in $CDCl_3$; spectra of acenaphthene chalconium salts were run in CD_3CN; δ (ppm), J (Hz).

dx.doi.org/10.1021/ic301627y | Inorg. Chem. 2012, 51, 11087–11097

Table 2. Selected Interatomic Distances (Angstroms) and Angles (degrees) for 2−14

	compd/+E(Me)Ph, Z						
	2/+S, SPh	**3**/+Se, SePh	**4**/+Te, SePh	**5**/+S, Br	**6**/+Se, Br	**7**/+Te, Br	**8**/+S, SPh
E(1)···Z(2); % Σr_{vdW}	3.006(2); 84	3.077(3); 81	3.177(1); 80	3.182(3) [3.181(3)]; 87 [87]	3.195(3); 85	3.2848(14); 84	3.093(3) [3.034(3)]; 86 [84]
E(1)−C(1)	1.801(4)	1.96(2)	2.136(11)	1.794(7) [1.789(11)]	1.943(11)	2.151(9)	1.797(6) [1.798(6)]
E(1)−C(13)	1.794(6)	1.953(13)	2.104(10)	1.801(9) [1.806(10)]	1.931(11)	2.124(10)	1.809(6) [1.804(6)]
E(1)−C(19)	1.808(4)	1.90(2)	2.147(13)	1.804(12) [1.797(11)]	1.945(12)	2.110(19)	1.802(8) [1.816(8)]
Z(2)−C(9)	1.779(4)	1.928(19)	1.943(11)	1.895(7) [1.928(11)]	1.893(11)	1.918(10)	1.769(6) [1.771(6)]
Σ of bay angles	373.5(8)	374.2(32)	373.1(23)	377.2(15) [376.3(16)]	377.8(22)	377.2(19)	374.8(13) [373.2(13)]
splay angle	13.5	14.2	13.1	17.2 [16.3]	17.8	17.2	14.8 [13.2]
Z(2)−E(1)−C(19)	100.65(1)	177.14(1)	171.23(1)	167.89(1) [166.14(1)]	176.30(1)	168.27(1)	173.37(1) [170.32(1)]
E(1)	−0.187(1)	0.206(1)	−0.525(1)	0.306(1) [-0.096(1)]	−0.116(1)	0.358(1)	0.229(1) [-0.215(1)]
Z(2)	0.200(1)	0.104(1)	0.469(1)	−0.091(1) [0.118(1)]	0.121(1)	−0.167(1)	−0.295(1) [0.270(1)]
C:(6)−(5)−(10)−(1)	−177.23(1)	−177.82(1)	−174.45(1)	178.53(1) [177.52(1)]	−179.15(1)	179.77(1)	174.07(1) [177.63(1)]
C:(4)−(5)−(10)−(9)	−176.01(1)	177.00(1)	−176.39(1)	176.53(1) [-178.21(1)]	−179.30(1)	178.01(1)	175.75(1) [175.92(1)]

	compd/+E(Me)Ph, EPh					
	9/+Se, SePh	**10**/+Te, TePh	**11**/+Se, SPh	**12**/+Te, SPh	**13**/+Te, SePh	**14**/+Te, +Te
E(1)···E(2); % Σr_{vdW}	3.2469(19); 85	3.445(3); 84	3.114(3) [3.073(4)]; 84 [83]	3.117(3); 81	3.2089(14) [3.1718(14)]; 81 [80]	3.5074(16)
E(1)−C(1)	1.956(5)	2.153(10)	1.936(9) [1.935(9)]	2.145(8)	2.132(9) [2.139(8)]	2.136(10)
E(1)−C(13)	1.944(5)	2.112(10)	1.937(11) [1.944(10)]	2.131(9)	2.103(9) [2.116(9)]	2.097(11)/2.152(12)
E(1)−C(19)	1.947(5)	2.161(9)	1.951(11) [1.940(13)	2.136(8)	2.131(11) [2.108(12)]	2.119(13)/2.118(13)
E(2)−C(9)	1.909(6)	2.108(11)	1.795(10) [1.805(10)]	1.780(8)	1.912(9) [1.927(9)]	2.136(10)
Σ of bay angles	376.8(11)	379.9(19)	374.2(19) [373.4(21)]	373.4(16)	376.8(18) [375.0(18)]	383.4(20)
splay angle	16.8	19.9	14.2 [13.4]	13.4	16.8 [15.0]	23.4
E(2)−E(1)−C(19)	176.71(1)	172.92(1)	178.94(1) [178.53(1)]	170.03(1)	171.10(1) [171.67(1)]	160.47(1)
E(1)	0.292(1)	−0.432(1)	−0.199(1) [0.186(1)]	0.262(1)	−0.143(1) [0.110(1)]	0.193(1)
E(2)	−0.366(1)	0.388(1)	0.262(1) [-0.267(1)]	−0.192(1)	0.227(1) ['-0.210(1)]	−0.238(1)
C:(6)−(5)−(10)−(1)	177.01(1)	174.51(1)	173.95(1) [176.41(1)]	175.09(1)	−176.97(1) [175.86(1)]	177.56(1)
C:(4)−(5)−(10)−(9)	177.20(1)	−175.48(1)	−175.86(1) [178.44(1)]	176.44(1)	−177.01(1) [179.81]	175.83(1)

dx.doi.org/10.1021/ic301627y | Inorg. Chem. 2012, 51, 11087−11097

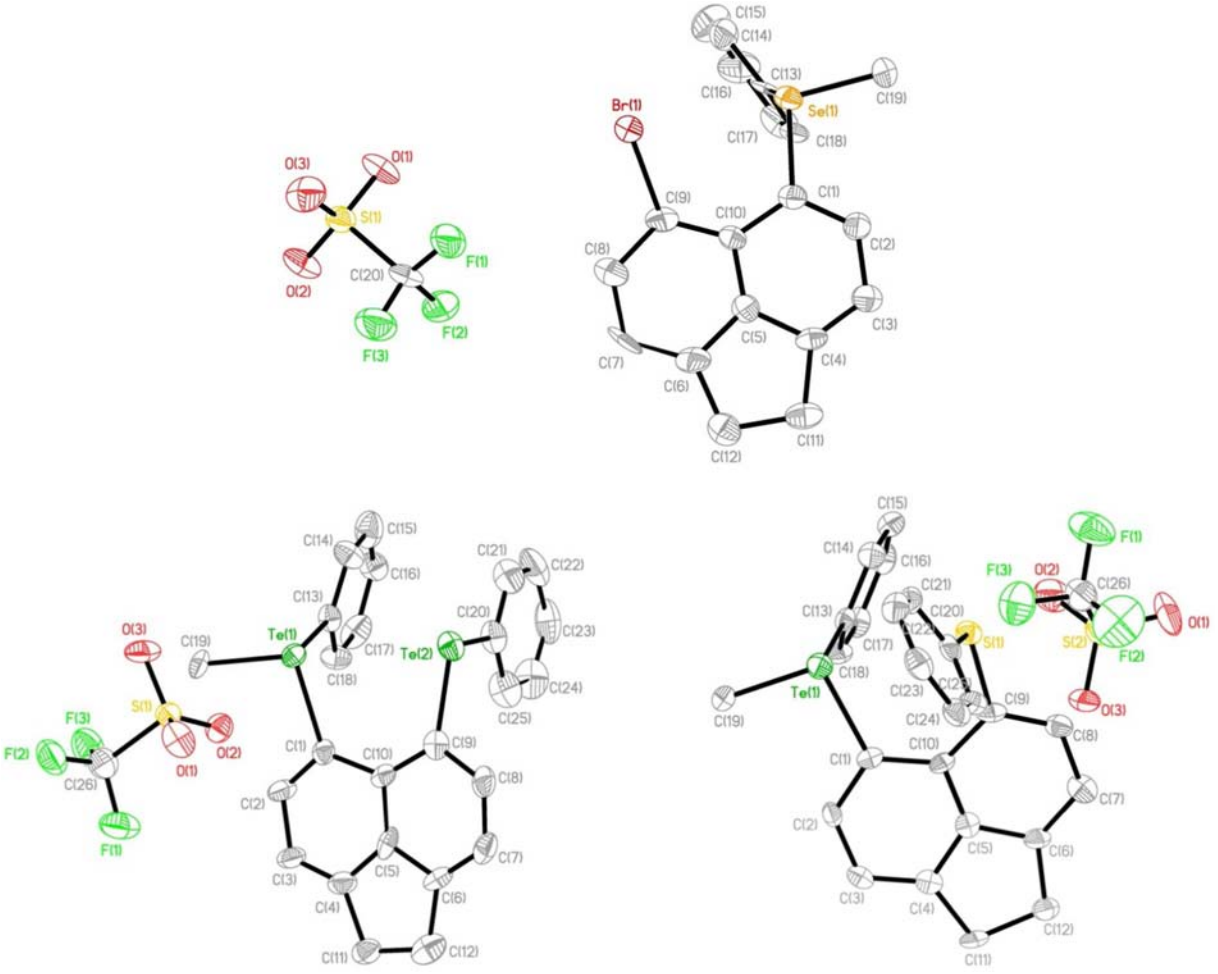

Figure 2. Thermal ellipsoid plots (50% probability) of chalconium salts **6**, **10**, and **12** (H atoms omitted for clarity). Structures of **5**, **7**, **8**, **9**, **11**, and **13** (adopting conformations similar to **6**, **10**, and **12**) are omitted here but can be found in the Supporting Information (Figure S4).

Solid-state NMR spectra were recorded for compounds **A9**−**A13** and **9**−**13**, and chemical shifts are found to be close to the solution-state values. It was not possible to determine *J* values owing to the larger line widths obtained in the solid-state NMR spectra. Deviations of up to 17.8 ppm for ^{77}Se and 62.8 ppm for ^{125}Te between the solution-state and the solid-state chemical shifts result from the changes in geometry imposed by the crystal structure in the solid state. DFT calculations of ^{77}Se and ^{125}Te NMR parameters were performed on fully geometry-optimized structures (full details are given in the Supporting Information). These enabled assignment of solid-state NMR spectra which contain more than one resonance. For compounds **A9** and **A10**, the two chemically equivalent selenium and tellurium atoms in each of the molecules are crystallographically inequivalent in the solid state owing to the conformation of the molecule. This results in the observation of two ^{77}Se and ^{125}Te distinct resonances in the solid-state NMR spectra for each compound. For the crystallographically inequivalent sites in these compounds, the experimental chemical shift differences of 51.6 (^{77}Se) and 114.3 ppm (^{125}Te) for **A9** and **A10** show reasonable agreement with differences of 35.5 and 135.6 ppm predicted by the calculations. Crystal structures of compounds **11** and **13** contain two crystallographically distinct molecules per asymmetric unit. For compound **11**, only one isotropic resonance was observed in the ^{77}Se solid-state NMR spectrum. We note that the two distinct selenium species in the structure have very similar local bonding geometries, and DFT calculations predict only a 7.5 ppm difference in chemical shift between the two sites.

Furthermore, DFT calculations performed on a structure for which only hydrogen positions were optimized predict a smaller chemical shift difference of 3.8 ppm. Therefore, it is likely that the two distinct selenium sites are unresolved in the experimental solid-state ^{77}Se NMR spectrum, where a line width of 5 ppm was obtained. For compound **13**, two ^{77}Se and two ^{125}Te resonances are observed in the experimental solid-state ^{77}Se and ^{125}Te NMR spectrum, indicating larger structural differences between the two molecules in the asymmetric unit.

This could be related to the larger difference in phenyl ring conformation between the two molecules in the crystal structure for **13** (Table S2, Supporting Information), which is known to be an important factor in determining ^{77}Se chemical shifts.[24,25] Indeed, the structural differences between the two crystallographically distinct molecules are reflected in the DFT calculations, which predict chemical differences of 19.0 (^{77}Se) and 10.7 ppm (^{125}Te).

X-ray Investigations. Suitable single crystals were obtained for **2** and **4** by slow evaporation of a dichloromethane solution of the product. Crystals for **3** and **5**−**14** were obtained by diffusion of hexane into saturated solutions of the individual compound in dichloromethane. Compounds **5**, **8**, **11**, and **13** contain two nearly identical molecules in the asymmetric unit,

dx.doi.org/10.1021/ic301627y | *Inorg. Chem.* 2012, 51, 11087−11097

in contrast to the remaining members of the series which crystallize with one molecule in the asymmetric unit. Selected interatomic bond lengths and angles are listed in Table 2. Further crystallographic information can be found in the Supporting Information.

The molecular structures of chalconium monocation salts **2**−**13** exhibit a range of structurally diverse configurations which are notably different from those of the respective parent derivatives **N2**−**N4**[17] and **A5**−**A13**.[21] As we previously reported,[17,21] the conformation of the aromatic ring systems and alignment of the aryl moieties dictates the final solid-state structure, influencing the degree of repulsion between p-type lone pairs (and hence the extent of molecular distortion) and enabling attractive intramolecular peri interactions to occur under appropriate geometric conditions. Similar to their parent precursors,[17,21] the absolute configuration of these systems can be classified by the relative alignment of the naphthalene and acenaphthene backbones and the aryl moieties with respect to the C(ar)−E−C(ar) planes (see Figures S2 and S3 and Tables S2 and S3, Supporting Information).[11,17,19,21,26]

The series of 5-bromo-6-(methyl)(phenyl)chalconium acenaphthenes **5**−**7** adopt the same equatorial−axial arrangement (Figures 2 and S3, Supporting Information), in each case positioning the E−C_{Me} bond along the mean acenaphthene plane and subsequently forcing the E−C_{Ph} bond to lie with a perpendicular configuration (type B-A; Figure S3, Supporting Information).[11,17,19,21,26] The location of the methyl functionality provides the correct geometry for the existence of a quasi-linear three-body Br···E−C_{Me} fragment with potential 3c-4e character[11,21] (Br···E−C angles (ψ) in the range 166−176°; Figure S3, Supporting Information). Naturally, the nonbonded Br···E peri distances increase with increasing chalcogen size, with separations lengthening from 3.181(3) Å [3.182(3) Å] in **5** to 3.2848(14) Å in **7** but still 13−16% shorter than the sum of van der Waals radii (Σr_{vdW}) in each case. The natural bond stretching and angle widening distortions of the acenaphthene framework are insufficient to completely alleviate the steric strain imposed by substitution of the bulky chalcogen and halogen substituents in **5**−**7**. Supplementary displacement of the peri atoms away from the acenaphthene mean plane and a greater divergence of the exocyclic bonds transpire to help alleviate peri space crowding. Considerable distortion is observed within the bay region, with large but comparable angular splays observed for the E−C_{Acenap} and X−C_{Acenap} bonds [**5** 17.2° [16.3°]; **6** 17.8°; **7** 17.2°]. The disposition of the peri atoms to opposite sides of the acenaphthene ring ranges from 0.1 to 0.9 Å, and further deformation is achieved by a minor buckling of the acenaphthene framework in each case (central torsion angles 1−4°).

Methylation of bis-chalcogen compounds **A8**−**A10** and mixed-chalcogen derivatives **A11**−**A13** affords a series of comparable structures in which the E−C_{Me} bond aligns along the plane of the acenaphthene backbone, similar to **5**−**7**. In each case the two phenyl rings are located perpendicular to the acenaphthene plane but with either a cis (**9**, **10**) or a trans (**8**, **11**−**13**) orientation (B-AA*c*/B-AA*t*; Figures 2 S3 and S4, Supporting Information). This promotes a quasi-linear E···E′−C_{Me} three-atom fragment which may promote delocalization of a chalcogen lone pair (G) to the antibonding σ^* (E−C) orbital, thus providing an attractive three-center four-electron (3c-4e) type component for the E···E′ interaction.[11,21] Evidence for this is supported by E···E′−C_{Me} angles (ψ) approaching 180° (170−177°) and short nonbonded peri distances, 16−19% within the sum of van der Waals radii for the two interacting chalcogen atoms (**8** 3.093(3) Å [3.034(3) Å]; **9** 3.2469(19) Å; **10** 3.445(3) Å; **11** 3.114(3) Å [3.073(4) Å]; **12** 3.117(3) Å; **13** 3.2089(14) Å [3.1718(14) Å]). In line with parent compounds **A8**−**A13**,[21] deformation of the natural acenaphthene geometry in **8**−**13** through in-plane and out-of-plane distortions and buckling of the carbon skeleton generally increases as larger atoms occupy the proximal 5,6 positions. A notable increase in the peri separation is observed as the heavier congeners are substituted, with a marked lengthening from 3.093(3) Å [3.034(3) Å] in **8** (Σr_{vdW} 3.60 Å)[27] to 3.445(3) Å in **10** (Σr_{vdW} 4.12 Å).[27] Naturally, the increased congestion of the peri space causes a greater divergence of the E−C_{Acenap} bonds within the acenaphthene plane, with large positive splay angles in the range 13.2−19.9°. This is accompanied by further displacement of the peri atoms to opposite sides of the mean acenaphthene plane (0.1−0.4 Å) and a reduction in the planarity of the organic framework by 1−6°.

Nevertheless, it is interesting to note that the small modification in orientation between the cis and the trans configurations of the axial phenyl rings in B-AA-type compounds (**8**−**13**) greatly affects the degree to which the chalcogen frontier orbitals take part in attractive or repulsive interactions. Despite an attractive 3c-4e-type interaction being present in each compound, irregular nonbonded B-AA*t* peri separations (**8**, **11**−**13**) are observed with respect to the size of the interacting atoms when compared with B-AA*c* (**9**, **10**) and B-A (**5**−**7**) systems (see Figure S6, Supporting Information), similar to the trends observed for the parent species (type A/AA vs B/AB).[21] Greater lone pair−lone pair repulsion is observed in compounds adopting type B-AA*c* and B-A configurations, with larger than expected peri distances compared to B-AA*t* systems where lone pair interactions are less effective. This is highlighted by the Se···Se peri distance in **9** (B-AA*c*) [3.2469(19) Å; Σr_{vdW} 3.80 Å[27]] being longer than the Te···E distances found in **12** (B-AA*t*) [3.117(3) Å; Σr_{vdW} 3.86 Å[27]] and **13** (B-AA*t*) [3.2089(14) Å (3.1718(14) Å); Σr_{vdW} 3.96 Å[27]], accommodating heavier chalcogen congeners. Similarly, the S···Br distance in **5** (B-A) [3.182(3) Å (3.181(3) Å); Σr_{vdW} 3.65 Å[27]] is longer than the Se···S distance in **11** (B-AA*t*) [3.114(3) Å (3.073(4) Å); Σr_{vdW} 3.70 Å[27]] and the Te···Br distance in **7** (B-A) [3.2848(14) Å; Σr_{vdW} 3.91 Å[27]] is longer than the Te···Se distance in **13** (B-AA*t*) [3.2089(14) Å (3.1718(14) Å); Σr_{vdW} 3.96 Å[27]]. Nevertheless, B-AA*c*- and B-A-type species behave as a related series, displaying a quasi-linear relationship between peri distance versus collective peri atom size (sum of van der Waals radii of the two peri atoms), with an expected general increase in peri separation as larger halogen or chalcogen congeners occupy the proximal 5,6 positions (Figure S6, Supporting Information).[21] A similar relationship is found for the series of compounds adopting the B-AA*t* motif. To complement these findings, DFT calculations were performed for acenaphthene derivatives **8**−**13**, comparing the cis and trans B-AA-type conformations and determining the extent of three-center, four-electron-type interactions occurring in the series (vide infra).

Interestingly, the three naphthalene compounds **2**−**4** adopt different configurations compared to their acenaphthene analogues (**8**, **9**, and **13**). In bis-selenide **3** (Figures S3 and S5, Supporting Information), minor rotation around the Se(9)−C(9) bond results in a twist orientation of the respective phenyl ring, affording a B-AC*c* configuration (cf. B-AA*c* adopted by acenaphthene **9**), while in naphthalene **4**

dx.doi.org/10.1021/ic301627y | *Inorg. Chem.* 2012, 51, 11087−11097

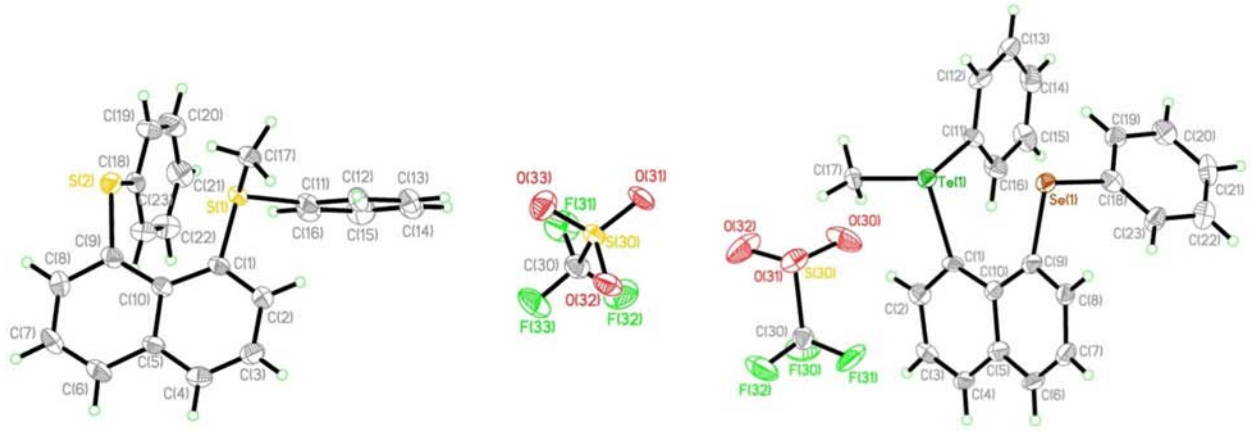

Figure 3. Thermal ellipsoid plots (50% probability) of naphthalene chalconium salts **2** and **4**. Structure of **3** is omitted here but can be found in Figure S5, Supporting Information.

(Figures 3, Supporting Information) the phenyl rings prefer to align with a cis orientation (B-AA*c*), contrasting with the trans configuration adopted by **13** (B-AA*t*). In both cases, the equatorial methyl group completes a quasi-linear E···E′−C_{Me} fragment, similar to acenaphthenes **8**−**13**, with short nonbonded peri distances, ∼20% shorter than the respective sum of van der Waals radii [**3** 3.077(3) Å; **4** 3.177(1) Å] and E···E′−C_{Me} angles which approach 180° [**3** ψ = 177.1°; **4** ψ = 171.2°].

The greatest disparity is observed in naphthalene **2** (Figures 3, Supporting Information) which adopts a C-CA*c* configuration (cf. **8** B-AA*t*) and is subsequently the only compound of those studied in this project that does not align the E−C_{Me} bond along the plane of the backbone. Subsequently, no linear fragment is found in **2**, with the C-CA*c* conformation accounting for a more acute S(2)···S(1)−C(17) angle of ψ = 100.7° and a larger relative peri separation than might be expected from interactions between lighter Group 16 congeners [3.006(2) Å: 84%].

Typically, naphthalene salts **2**−**4** display less molecular distortion and shorter peri distances compared with analogous acenaphthene derivatives **8**, **9**, and **13**,[21] although significant deformation of the naphthalene geometry is still required in order to accommodate the large chalcogen atoms. Elongation of the C−C bonds around C10 (mean 1.43 Å; cf. C5 bonds 1.42 Å) is supplemented by an increase in the C1−C10−C9 angular splay (mean 127°; cf. C4−C5−C6 120°). Additional relaxation is afforded by the displacement of the peri atoms to opposite sides of the naphthyl plane (0.2−0.5 Å) and the divergence of the exocyclic bonds (splay angles 13.1−14.2°). Considerable buckling of the usually rigid naphthalene unit is also observed with central C−C−C−C torsion angles deviating from planarity by 2−6°.

Treatment of 5,6-bis(phenyltelluro)acenaphthene **A13** with 2 mol equiv of MeOTf resulted in methylation of both tellurium centers, affording the dication salt [{Acenap-$(TePh)_2(Me)_2$}$^{2+}$$(OTf^-)_2$] **14** (Figure 4). The additional electrostatic repulsion acting between the positively charged cationic tellurium centers enhances the steric strain within the peri region and leads to a greater deformation of the acenaphthene carbon framework compared with monocation **10**. The repulsive Te^+···Te^+ Coulombic interaction is predominantly accommodated by a greater in-plane divergence of the exocyclic Te−C_{Acenap} bonds [splay angle for **14** 23.4° and **10** 19.9°], which leads to an increase in the nonbonding

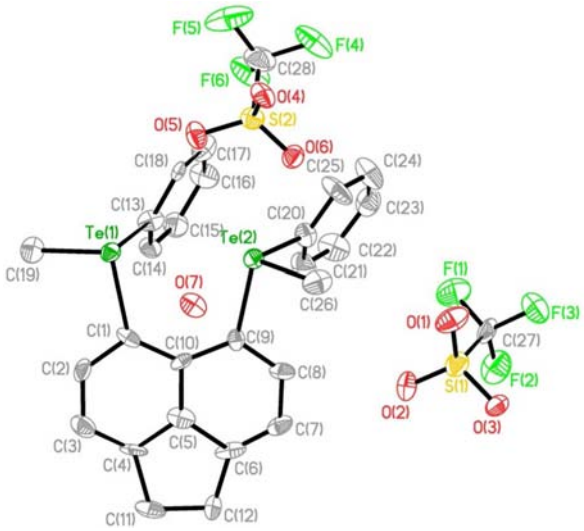

Figure 4. Thermal ellipsoid plot (50% probability) of dication chalconium salt **14** (H atoms omitted for clarity).

Te^+···Te^+ separation [3.5074(16) Å] compared with the telluronio−tellurenyl Te^+···Te separation in monocation **10** [3.445(3) Å]. Nevertheless, the Te^+···Te^+ separation in **14** [3.5074(16) Å] is still 15% shorter than twice the van der Waals radii for Te [4.12 Å].[27]

The conformation of dication **14** can be classified as type C-CC*c*-C (Figures 4 and S3, Supporting Information). The two Te−C_{Me} bonds are displaced 151.14(1)° and 136.01(1)° from the respective C(10)−C(1)−Te−C_{Me} planes (Table S3, Supporting Information), locating the methyl groups at positions between an equatorial and an axial configuration, corresponding to a twist conformation. The two methyl groups subsequently point away from the center of the molecule and are located on opposite sides of the acenaphthene ring. Amassing the bulk of the substituents on one side of the molecule (top half in Figure 5) leaves much open space on the other. In the solid, this space is actually occupied by a water molecule (see O(7) Figure 4), presumably introduced during workup in air. Crystallization under anhydrous conditions affords the same structure of the dication of **14**, now with an O atom from one of the triflate counterions at the position of this water (the "anhydrous" structure still contains one water

dx.doi.org/10.1021/ic301627y | *Inorg. Chem.* 2012, 51, 11087−11097

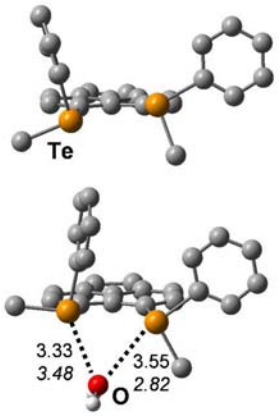

Figure 5. B3LYP-optimized bare dication from **14** (top) and with one water molecule added (bottom), including selected bond distances in Angstroms (italics, from X-ray crystallography); organic H atoms omitted for clarity.

molecule per two structural units, but this is more remote from the Te atoms).

DFT Calculations. To assess the role of the water molecule in **14**, density functional theory (DFT) calculations were performed. When an optimization is started for the pristine dication from the crystal structure, a B-AB-A-type minimum is obtained (top of Figure 5), reminiscent of related neutral bis(phosphines).[28] When the water molecule is retained, a noticeably different conformation is obtained (bottom of Figure 5), about halfway between the pristine minimum and the structure observed in the solid (note that dispersion forces favoring π stacking are not accounted for at the level used).

The water is held in a position not too far from where it is found in the solid, though not approaching the Te atoms quite as closely (see the distances on the bottom of Figure 5). In the starting structure, one of the H atoms of the water (which were not refined in X-ray analysis) was placed pointing toward the lone pair of the more distant Te atom but rotated away during optimization. In the gas phase, this water molecule is bound rather strongly (with a raw binding energy exceeding 40 kcal/mol at the B3LYP level) and mostly through electrostatic interactions between the positively charged Te atoms (+1.4e according to natural population analysis) and the negatively charged O atom.

Additional DFT calculations were performed for acenaphthene derivatives **8**−**13**, comparing the cis and trans B-AA-type conformations and determining the extent of three-center, four-electron-type interactions occurring in the series. Selected geometrical parameters for **8**−**13** together with the chalcogen−chalcogen Wiberg bond indices (WBIs)[29] are collated in Table S9, Supporting Information. The latter are a probe for the extent of covalent bonding, approaching a value close to one for true single bonds.

Atomic coordinates obtained from X-ray crystallography were reoptimized at the B3LYP level to ensure that the chosen basis sets and effective core potentials (ECPs) are adequate for the problem at hand. Interestingly, the optimized peri distances between the chalcogens are noticeably shorter than those observed in the solid, by up to 0.08 Å (overestimation is usually a common DFT problem). Nevertheless, this appears systematic as an excellent linear correlation is found between DFT and X-ray distances, with a slope of 0.88 and a correlation coefficient of 0.96 (Figure S7, Supporting Information).

In order to assess the difference between the cis and the trans structural motifs, a conformational search was undertaken where all molecules **8**−**13** were optimized in the respective other conformation. In each case the two possible B-AA conformations were considered, with the phenyl groups adopting either the cis (B-AA*c*) or the trans (B-AA*t*) orientation. It is interesting to note that AA*c* conformations could be optimized for all members of the group, contrasting with a similar study of the parent compounds **A8**−**A13** which invariably optimized to AB forms (or intermediate structures denoted AC or CC, where one or both of the dihedral angles θ are close to 140°; Figure S2, Supporting Information).

In all cases the most stable conformer corresponded to the B-AA*t* configuration, but the energy span between the two conformations is remarkably small, ranging from 3.7 kJ/mol for **8** to 7.1 kJ/mol for **10** (Table S9, Supporting Information). Formation of the B-AA*c* conformer for **9** and **10** in the solid is likely to be due to intermolecular interactions or packing forces. When the phenyl substituents are moved from a cis orientation to a trans orientation, a small decrease in the peri distance is observed. The extent of this decrease ranges from 0.002 Å for **8** to 0.031 Å for **10** (Table S9, Supporting Information) and is more pronounced as the size of the interacting peri atoms increases. The extent of covalent bonding in **8**−**13** was investigated to assess whether the change in peri distance with conformation is a result of specific bonding interactions. The Wiberg bond index (WBI), which usually approaches a value of one for a true single bond, was investigated for each conformer in the series (**8**−**13**).

In general, there is a trend to higher WBIs as large atoms occupy the proximal peri positions, independent of the conformation of the aromatic rings. In all cases, WBIs for the B-AA*t* conformer are slightly greater than for the equivalent B-AA*c* structure by 0.004−0.011 units. As expected, very small WBIs (0.052/0.041) are computed for the two conformers of **8** with a relatively large peri distance (86% Σr_{vdW}) between the two small sulfur substituents. Significantly higher values are obtained for the heavier members of the series with WBIs in the range from 0.102 (**9** SeSe) to 0.184 (**10** TeTe), indicating the onset of weak three-center, four-electron-type interactions, which become more prevalent as heavier congeners are introduced along the series. In the second-order perturbation analysis of the natural bond orbitals (NBOs)[30] of **10**, weak donor−acceptor interactions are apparent, involving the p-type lone pair on the TePh group and the σ^*(Te-CH_3) antibonding orbital on the other side. These interactions amount to ca. 60 kJ/mol, similar to the findings for the neutral precursor **A10**.[21] Unsurprisingly, significantly lower WBIs are obtained for the dication **14** (0.046) and its water adduct (0.039), cf. Figure 5.

These findings correlate with the ^{77}Se and ^{125}Te NMR data and *J* coupling values. Considering the ^{125}Te solid-state chemical shifts for compounds **10**, **12**, and **13**, a systematic decrease in chemical shift of the Te^+ species is observed as heavier congeners are introduced on the adjacent peri site. This indicates that as the adjacent atom becomes heavier, the Te^+ species becomes more shielded due to increasing through-space lone pair interactions between the two chalcogen congeners. Similarly, the ^{77}Se chemical shift for the Se^+ species in compound **9** is also lower than that for compound **11**, indicating that through-space interactions are increased for compound **9**, which contains the heavier congener on the adjacent peri site. These observations are mirrored in the ^{77}Se and ^{125}Te solution-state NMR chemical shifts, which follow the

dx.doi.org/10.1021/ic301627y | *Inorg. Chem.* 2012, 51, 11087−11097

same trend, and evidence for through-space interactions is supported by the J coupling values, which are substantially larger for compounds containing heavier chalcogen pairs.

CONCLUSION

Naphthalene compounds **N2**−**N4**[17] and associated acenaphthene derivatives **A5**−**A13**[21] have been independently treated with MeOTf, affording 12 monocation chalconium salts **2**−**13**. Reaction of bis-tellurium compound **A10** with 2 equiv of MeOTf additionally afforded the doubly methylated dication salt $[\{Acenap(TePhMe)_2\}^{2+}\{(CF_3SO_3)_2\}^{2-}]$ **14**. Where a choice exists between potential methylation sites (mixed-chalcogen derivatives, bromo−chalcogen species) reaction occurs preferentially at the least electronegative chalcogen atom or exclusively at the chalcogen atom in the case of the bromine compounds. The molecular structures of **2**−**13** adopt a variety of conformations which are notably different than their parent derivatives. While a general increase in the peri distance is observed when larger atoms occupy the proximal peri positions, the conformation of the aromatic rings and subsequent location of p-type lone pairs has a significant impact on the geometry of the peri region, with anomalies in peri separations correlated to the ability of the frontier orbitals to take part in attractive or repulsive interactions. Compounds adopting type B-AA*c* and B-A configurations experience greater lone pair−lone pair repulsion and consequently exhibit larger than expected peri distances relative to the size of the interacting atoms compared to B-AA*t* systems. In the majority of cases, an equatorial alignment of the E−C_{Me} bond affords a quasi-linear three-body C_{Me}−E···Z (E = Te, Se, S; Z = Br/E) fragment, providing an attractive component for the E···Z interaction. Density functional studies confirmed these interactions and suggested the onset of three-center, four-electron-type bonding under appropriate geometric conditions, becoming more prevalent as heavier congeners occupy the proximal peri positions. These findings correlate with the ^{77}Se and ^{125}Te NMR data and J coupling values.

EXPERIMENTAL SECTION

All experiments were carried out under an oxygen- and a moisture-free nitrogen atmosphere using standard Schlenk techniques and glassware. Reagents were obtained from commercial sources and used as received. Dry solvents were collected from a MBraun solvent system. Elemental analyses were performed by the University of St. Andrews School of Chemistry Microanalysis Service. Infrared spectra were recorded as KBr discs in the range 4000−300 cm^{-1} on a Perkin-Elmer System 2000 Fourier transform spectrometer. ^{1}H and ^{13}C NMR spectra were recorded on a Jeol GSX 270 MHz spectrometer with δ(H) and δ(C) referenced to external tetramethylsilane. ^{77}Se and ^{125}Te NMR spectra were recorded on a Jeol GSX 270 MHz spectrometer with δ(Se) and δ(Te) referenced to external Me_2Se and Me_2Te, respectively, with a secondary reference for δ(Te) to diphenyl ditelluride (δ(Te) = 428 ppm). ^{19}F NMR spectra were recorded on a Bruker Ultrashield 400 MHz spectrometer with δ(F) referenced to external trichlorofluoromethane. Assignments of ^{13}C and ^{1}H NMR spectra were made with the help of H−H COSY and HSQC experiments. All measurements were performed at 25 °C. All values reported for NMR spectroscopy are in parts per million (ppm). Coupling constants (J) are given in Hertz (Hz). Mass spectrometry was performed by the University of St. Andrews Mass Spectrometry Service. Electron impact mass spectrometry (EIMS) and Chemical Ionization Mass Spectrometry (CIMS) was carried out on a Micromass GCT orthogonal acceleration time-of-flight mass spectrometer. Electrospray mass spectrometry (ESMS) was carried out on a Micromass LCT orthogonal accelerator time-of-flight mass spectrometer.

$[\{Nap(SPh_2)Me\}^+\{CFSO_3\}^-]$ (2). To a solution of 1,8-bis-(phenylsulfanyl)naphthalene (0.38 g, 1.11 mmol) in dichloromethane (20 mL) was added methyl trifluoromethanesulfonate (0.13 mL, 1.11 mmol) at room temperature. The reaction mixture was stirred at this temperature for 24 h, and the solvent was removed in vacuo. The crude product was washed with diethyl ether, and the brown precipitate which formed was collected by filtration. An analytically pure sample was obtained by slow evaporation of a dichloromethane solution of the product (0.45 g, 80%); mp 82−84 °C. ^{1}H NMR (270 MHz, $CDCl_3$, 25 °C, TMS) δ = 8.19 (1 H, d, ^3J (H,H) = 7.9, Nap 4-H), 8.06 (1 H, dd, ^3J (H,H) = 8.3, ^4J (H,H) = 1.2, Nap 5-H), 8.02 (1 H, dd, ^3J (H,H) = 7.8, ^4J (H,H) = 1.0, Nap 2-H), 7.95 (1 H, dd, ^3J (H,H) = 7.2, ^4J (H,H) = 1.3, Nap 7-H), 7.71 (1 H, t, ^3J (H,H) = 7.9, Nap 3-H), 7.59 (1 H, t, ^3J (H,H) = 7.8, Nap 6-H), 7.45−7.38 (5H, m, S^+Ph 12−16-H), 7.12−7.00 (3 H, m, SPh 19−21-H), 6.73−6.68 (2 H, m, $SePh$ 18,22-H), 3.48 (3 H, s, CH_3). ^{19}F NMR (376.5 MHz, $CDCl_3$, 25 °C, CCl_3F): −78.79(s). MS (ES^+): m/z (%) 358.89 (100) [M^+ − OTf].

$[\{Nap(SePh_2)Me\}^+\{CFSO_3\}^-]$ (3). Compound **3** was synthesized by the method described for **2** but with $[Nap(SePh)_2]$ (0.14 g, 0.31 mmol) and MeOTf (0.04 mL, 0.31 mmol). An analytically pure sample was obtained by recrystallization from diffusion of pentane into a saturated dichloromethane solution of the product (0.17 g, 88%); mp 94−96 °C. ^{1}H NMR (270 MHz, $CDCl_3$, 25 °C, TMS) δ = 8.25 (1 H, d, ^3J (H,H) = 7.9, Nap 4-H), 8.17 (1 H, d, ^3J (H,H) = 8.9, Nap 5-H), 8.15 (1 H, d, ^3J (H,H) = 10.0, Nap 7-H), 7.98 (1 H, d, ^3J (H,H) = 7.3, Nap 2-H), 7.76 (1 H, t, ^3J (H,H) = 7.9, Nap 3-H), 7.64 (1 H, t, ^3J (H,H) = 7.9, Nap 6-H), 7.50−7.38 (5H, m, Se^+Ph 12−16-H), 7.16−7.08 (3 H, m, $SePh$ 19−21-H), 6.98−6.86 (2 H, m, $SePh$ 18,22-H), 3.32 (3 H, s, ^2J (H,Se) = 14.1 Hz, CH_3). ^{77}Se NMR (51.5 MHz, $CDCl_3$, 25 °C, Me_2Se): δ = 436 (s, ^4J (Se,Se) = 167), 392 (s, ^4J (Se,Se) = 167). ^{19}F NMR (376.5 MHz, $CDCl_3$, 25 °C, CCl_3F): −78.75(s). MS (ES^+): m/z (%) 454.54 (100) [M^+ − OTf].

$[\{Nap(TePh)(SePh)Me\}^+\{CFSO_3\}^-]$ (4). Compound **4** was synthesized by the method described for **2** but with [Nap(TePh)(SePh)] (0.10 g, 0.20 mmol) and MeOTf (0.02 mL, 0.20 mmol). An analytically pure sample was obtained by slow evaporation of a dichloromethane solution of the product (0.11 g, 89%); mp 130−132 °C. ^{1}H NMR (270 MHz, $CDCl_3$, 25 °C, TMS) δ = 8.15−8.08 (2 H, m, Nap 4,5-H), 8.05 (1 H, d, ^3J (H,H) = 8.2, Nap 2-H), 7.74 (1 H, d, ^3J (H,H) = 7.4, Nap 7-H), 7.61−7.49 (2 H, m, Nap 3,6-H), 7.47−7.37 (3 H, m, Te^+Ph 11−13-H), 7.35−7.27 (2 H, m, Te^+Ph 10,14-H), 7.14−7.04 (3 H, m, $SePh$ 18−20-H), 6.94−6.84 (2 H, m, $SePh$ 17,21-H), 2.69 (3 H, s, ^2J (H,Te) = 30.5, CH_3). ^{77}Se NMR (51.5 MHz, $CDCl_3$, 25 °C, Me_2Se): δ = 347(s). ^{125}Te NMR (81.2 MHz, $CDCl_3$, 25 °C, PhTeTePh): δ = 706 (^4J (Te,Se) = 429). ^{19}F NMR (376.5 MHz, $CDCl_3$, 25 °C, CCl_3F): −78.69(s). MS (ES^+): m/z (%) 502.32 (100) [M^+ − OTf].

$[\{Acenap(Br)(SPh)Me\}^+\{CFSO_3\}^-]$ (5). Compound **5** was synthesized by the method described for **2** but with [Acenap(Br)(SPh)] (0.24 g, 0.72 mmol) and MeOTf (0.08 mL, 0.72 mmol). An analytically pure sample was obtained by recrystallization from diffusion of hexane into a dichloromethane solution of the product (0.32 g, 88%); mp 119−121 °C. ^{1}H NMR (270 MHz, CD_3CN, 25 °C, TMS) δ = 8.13 (1 H, d, ^3J (H,H) = 7.7, Acenap 4-H), 7.95 (1 H, d, ^3J (H,H) = 7.5, Acenap 7-H), 7.83−7.75 (2 H, m, S^+Ph 13,15-H), 7.75−7.71 (1 H, m, S^+Ph 14-H), 7.71−7.60 (3 H, m, Acenap 3-H, S^+Ph 12,16-H), 7.39 (1 H, d, ^3J (H,H) = 7.5, Acenap 8-H), 3.62 (3 H, s, CH_3), 3.55−3.35 (4 H, m, 2 × CH_2). ^{19}F NMR (376.5 MHz, CD_3CN, 25 °C, CCl_3F): −79.77(s). MS (ES^+): m/z (%) 354.91 (100) [M^+ − OTf]. Anal. Calcd for $C_{20}H_{16}BrF_3O_3S_2$: C, 47.5; H, 3.2. Found: C, 47.2; H, 3.0.

$[\{Acenap(Br)(SePh)Me\}^+\{CFSO_3\}^-]$ (6). Compound **6** was synthesized by the method described for **2** but with [Acenap(Br)-(SePh)] (0.27 g, 0.70 mmol) and MeOTf (0.08 mL, 0.70 mmol). An analytically pure sample was obtained by recrystallization from diffusion of hexane into a dichloromethane solution of the product (0.35 g, 90%); mp 150−152 °C. ^{1}H NMR (270 MHz, CD_3CN, 25 °C,

dx.doi.org/10.1021/ic301627y | Inorg. Chem. 2012, 51, 11087−11097

TMS) δ = 7.92 (2 H, d, ^3J (H,H) = 7.8, Acenap 4,7-H), 7.75−7.66 (3 H, m, Se$^+$*Ph* 13−15-H), 7.66−7.56 (3 H, m, Acenap 8-H, Se$^+$*Ph* 12,16-H), 7.40 (1 H, d, ^3J (H,H) = 7.6, Acenap 3-H), 3.55−3.41 (4 H, m, 2 × CH_2), 3.38 (3 H, s, ^2J (H,Se) = 13.2, CH_3). ^{77}Se NMR (51.5 MHz, CD_3CN, 25 °C, Me_2Se): δ = 420 (s). ^{19}F NMR (376.5 MHz, CD_3CN, 25 °C, CCl_3F): −79.77(s). MS (ES$^+$): *m*/*z* (%) 402.84 (100) [M$^+$ − OTf]. Anal. Calcd for $C_{20}H_{16}BrF_3O_3SSe$: C, 43.5; H, 2.9. Found: C, 43.1; H, 2.9.

[{Acenap(Br)(TePh)Me}$^+${CFSO$_3$}$^-$] (7). Compound **7** was synthesized by the method described for **2** but with [Acenap(Br)-(TePh)] (0.22 g, 0.50 mmol) and MeOTf (0.06 mL, 0.50 mmol). An analytically pure sample was obtained by recrystallization from diffusion of hexane into a dichloromethane solution of the product (0.26 g, 88%); mp 135−137 °C. ^{1}H NMR (270 MHz, CD_3CN, 25 °C, TMS) δ = 7.88 (1 H, d, ^3J (H,H) = 7.5, Acenap 4-H), 7.87 (1 H, d, ^3J (H,H) = 7.5, Acenap 7-H), 7.74−7.66 (2 H, m, Te$^+$*Ph* 12,16-H), 7.64−7.58 (1 H, m, Te$^+$*Ph* 14-H), 7.57−7.44 (3 H, m, Acenap 3-H, Te$^+$*Ph* 13,15-H), 7.37 (1 H, d, ^3J (H,H) = 7.5, Acenap 8-H), 3.52−3.44 (2 H, m, CH_2), 3.44−3.34 (2 H, m, CH_2), 2.86 (3 H, s, ^2J (H,Te) = 30.6, CH_3). ^{125}Te NMR (81.2 MHz, CD_3CN, 25 °C, PhTeTePh): δ = 693. ^{19}F NMR (376.5 MHz, CD_3CN, 25 °C, CCl_3F): −79.80(s). MS (ES$^+$): *m*/*z* (%) 452.77 (100) [M$^+$ − OTf]. Anal. Calcd for $C_{20}H_{16}BrF_3O_3STe$: C, 39.9; H, 2.7. Found: C, 40.1; H, 2.6.

[{Acenap(SPh)$_2$Me}$^+${CFSO$_3$}$^-$] (8). Compound **8** was synthesized by the method described for **2** but with [Acenap(SPh)$_2$] (0.25 g, 0.69 mmol) and MeOTf (0.08 mL, 0.69 mmol). An analytically pure sample was obtained by recrystallization from diffusion of hexane into a dichloromethane solution of the product (0.34 g, 92%); mp 107−109 °C. ^{1}H NMR (270 MHz, CD_3CN, 25 °C, TMS) δ = 8.05 (1 H, d, ^3J (H,H) = 7.3, Acenap 4-H), 7.95 (1 H, d, ^3J (H,H) = 7.7, Acenap 7-H), 7.69−7.60 (3 H, m, Acenap 3,8-H, S$^+$*Ph* 14-H), 7.60−7.43 (4 H, m, S$^+$*Ph* 12,13,15,16-H), 7.29−7.13 (3 H, m, S*Ph* 20−22-H), 6.95−6.85 (2 H, m, S*Ph* 19,23-H), 3.62−3.51 (4 H, m, 2 × CH_2), 3.47 (3 H, s, CH_3). ^{19}F NMR (376.5 MHz, CD_3CN, 25 °C, CCl_3F): −79.81(s). MS (ES$^+$): *m*/*z* (%) 384.95 (100) [M$^+$ − OTf]. Anal. Calcd for $C_{26}H_{21}F_3O_3S_3$: C, 58.4; H, 3.9. Found: C, 58.4; H, 3.8.

[{Acenap(SePh)$_2$Me}$^+${CFSO$_3$}$^-$] (9). Compound **9** was synthesized by the method described for **2** but with [Acenap(SePh)$_2$] (0.65 g, 1.39 mmol) and MeOTf (0.16 mL, 1.39 mmol). An analytically pure sample was obtained by recrystallization from diffusion of hexane into a dichloromethane solution of the product (0.80 g, 91%); mp 125−127 °C. ^{1}H NMR (270 MHz, CD_3CN, 25 °C, TMS) δ = 8.12 (1 H, d, ^3J (H,H) = 7.3, Acenap 4-H), 7.91 (1 H, d, ^3J (H,H) = 7.7, Acenap 7-H), 7.62 (1 H, d, ^3J (H,H) = 7.7, Acenap 8-H), 7.60−7.44 (6 H, m, Acenap 3-H, Se$^+$*Ph* 12−16-H), 7.22−7.11 (3 H, m, Se*Ph* 20−22-H), 7.07−6.97 (2 H, m, Se*Ph* 19,23-H), 3.58−3.47 (4 H, m, 2 × CH_2), 3.24 (3 H, s, ^2J (H,Se) = 13.6, CH_3). ^{77}Se NMR (51.5 MHz, CD_3CN, 25 °C, Me_2Se): δ = 422 (s, ^4J (Se,Se) = 141), 366 (s, ^4J (Se,Se) = 141). ^{19}F NMR (376.5 MHz, CD_3CN, 25 °C, CCl_3F): −79.74(s). MS (ES$^+$): *m*/*z* (%) 480.84 (100) [M$^+$ − OTf]. Anal. Calcd for $C_{26}H_{21}F_3O_3SSe_2$: C, 49.7; H, 3.4. Found: C, 49.5; H, 3.3.

[{Acenap(TePh)$_2$Me}$^+${CFSO$_3$}$^-$] (10). Compound **10** was synthesized by the method described for **2** but with [Acenap(TePh)$_2$] (0.24 g, 0.42 mmol) and MeOTf (0.05 mL, 0.42 mmol). An analytically pure sample was obtained by recrystallization from diffusion of hexane into a dichloromethane solution of the product (0.29 g, 95%); mp 155−157 °C. ^{1}H NMR (270 MHz, CD_3CN, 25 °C, TMS) δ = 8.47 (1 H, d, ^3J (H,H) = 7.1, Acenap 4-H), 7.91 (1 H, d, ^3J (H,H) = 7.5, Acenap 7-H), 7.65−7.58 (2 H, m, Te$^+$*Ph* 12,16-H), 7.58−7.51 (2 H, m, Acenap 8-H, Te$^+$*Ph* 14-H), 7.51−7.39 (3 H, m, Acenap 3-H, Te$^+$*Ph* 13,15-H), 7.27−7.18 (3 H, m, Te*Ph* 20−22-H), 7.18−7.10 (2 H, m, Te*Ph* 19,23-H), 3.60−3.47 (4 H, m, 2 × CH_2), 2.70 (3 H, s, ^2J (H,Te) = 33.1, CH_3). ^{125}Te NMR (81.2 MHz, CD_3CN, 25 °C, PhTeTePh): δ = 641(s, ^4J (^{125}Te,^{125}Te) 946), 522(s, ^4J (Te,Te) 946). ^{19}F NMR (376.5 MHz, CD_3CN, 25 °C, CCl_3F): −79.77(s). MS (ES$^+$): *m*/*z* (%) 576.78 (100) [M$^+$ − OTf]. Anal. Calcd for $C_{26}H_{21}F_3O_3STe_2$: C, 42.7; H, 2.9. Found: C, 42.8; H, 2.9.

[{Acenap(SePh)(SPh)Me}$^+${CFSO$_3$}$^-$] (11). Compound **11** was synthesized by the method described for **2** but with [Acenap(SePh)-(SPh)] (0.25 g, 0.60 mmol) and MeOTf (0.07 mL, 0.60 mmol). An analytically pure sample was obtained by recrystallization from diffusion of hexane into a dichloromethane solution of the product (0.34 g, 96%); mp 92−94 °C. ^{1}H NMR (270 MHz, CD_3CN, 25 °C, TMS) δ = 8.00 (1 H, d, ^3J (H,H) = 7.3, Acenap 4-H), 7.91 (1 H, d, ^3J (H,H) = 7.7, Acenap 7-H), 7.65 (1 H, d, ^3J (H,H) = 7.7, Acenap 8-H), 7.60 (1 H, d, ^3J (H,H) = 7.3, Acenap 3-H), 7.58−7.43 (5 H, m, Se$^+$*Ph* 12−16-H), 7.23−7.12 (3 H, m, S*Ph* 20−22-H), 6.94−6.85 (2 H, m, S*Ph* 19,23-H), 3.62−3.50 (4 H, m, 2 × CH_2), 3.20 (3 H, s, ^2J (H,Se) = 13.5, CH_3). ^{77}Se NMR (51.5 MHz, $CDCl_3$, 25 °C, Me_2Se): δ = 431 (s). ^{19}F NMR (376.5 MHz, CD_3CN, 25 °C, CCl_3F): −79.87(s). MS (ES$^+$): *m*/*z* (%) 432.84 (100) [M$^+$ − OTf].

[{Acenap(TePh)(SPh)Me}$^+${CFSO$_3$}$^-$] (12). Compound **12** was synthesized by the method described for **2** but with [Acenap(TePh)-(SPh)] (0.34 g, 0.72 mmol) and MeOTf (0.08 mL, 0.72 mmol). An analytically pure sample was obtained by recrystallization from diffusion of hexane into a dichloromethane solution of the product (0.42 g, 87%); mp 166−168 °C. ^{1}H NMR (270 MHz, CD_3CN, 25 °C, TMS) δ = 8.00 (1 H, d, ^3J (H,H) = 7.3, Acenap 4-H), 7.86 (1 H, d, ^3J (H,H) = 7.5, Acenap 7-H), 7.66−7.57 (4 H, m, Acenap 3,8-H, Te$^+$*Ph* 13,15-H), 7.57−7.51 (1 H, m, Te$^+$*Ph* 14-H), 7.50−7.41(2 H, m, Te$^+$*Ph* 12,16-H), 7.32−7.17 (3 H, m, S*Ph* 20−22-H), 6.96−6.87 (2 H, m, S*Ph* 19,23-H), 3.62−3.49 (4 H, m, 2 × CH_2), 2.66 (3 H, s, ^2J (H,Te) = 31.5, CH_3). ^{125}Te NMR (81.2 MHz, CD_3CN, 25 °C, PhTeTePh): δ = 694(s). ^{19}F NMR (376.5 MHz, CD_3CN, 25 °C, CCl_3F): −79.78(s). MS (ES$^+$): *m*/*z* (%) 482.86 (100) [M$^+$ − OTf]. Anal. Calcd for $C_{26}H_{21}F_3O_3S_2Te$: C, 49.6; H, 3.4. Found: C, 49.3; H, 3.1.

[{Acenap(TePh)(SePh)Me}$^+${CFSO$_3$}$^-$] (13). Compound **13** was synthesized by the method described for **2** but with [Acenap(TePh)-(SePh)] (0.10 g, 0.20 mmol) and MeOTf (0.03 mL, 0.20 mmol). An analytically pure sample was obtained by recrystallization from diffusion of hexane into a dichloromethane solution of the product (0.12 g, 92%); mp 138−140 °C. ^{1}H NMR (270 MHz, CD_3CN, 25 °C, TMS) δ = 8.13 (1 H, d, ^3J (H,H) = 7.2, Acenap 4-H), 7.87 (1 H, d, ^3J (H,H) = 7.5, Acenap 7-H), 7.65−7.50 (5 H, m, Acenap 3,8-H, Te$^+$*Ph* 12,14,16-H), 7.50−7.39 (2 H, m, Te$^+$*Ph* 13,15-H), 7.27−7.16 (3 H, m, Se*Ph* 20−22-H), 7.08−6.98 (2 H, m, Se*Ph* 19,23-H), 3.61−3.48 (4 H, m, 2 × CH_2), 2.66 (3 H, s, ^2J (H,Te) = 32.2, CH_3); ^{77}Se NMR (51.5 MHz, CD_3CN, 25 °C, Me_2Se): δ = 323(s, ^4J (Se,Te) = 382). ^{125}Te NMR (81.2 MHz, CD_3CN, 25 °C, PhTeTePh): δ = 679(s, ^4J (^{125}Te,Se) = 382). ^{19}F NMR (376.5 MHz, CD_3CN, 25 °C, CCl_3F): −79.85(s). MS (ES$^+$): *m*/*z* (%) 528.83 (100) [M$^+$ − OTf]. Anal. Calcd for $C_{26}H_{21}F_3O_3SSeTe$: C, 46.12; H, 3.13. Found: C, 46.25; H, 2.68.

[{Acenap(TePh)$_2$Me$_2$}$^{2+}${CFSO$_3$}$_2^{2-}$] (14). Compound **14** was synthesized by the method described for **2** but with [Acenap(TePh)$_2$] (0.28 g, 0.49 mmol) and MeOTf (0.22 mL, 1.97 mmol). An analytically pure sample was obtained by recrystallization from diffusion of hexane into a dichloromethane solution of the product (0.24 g, 54%); mp 115−117 °C. ^{1}H NMR (270 MHz, CD_3CN, 25 °C, TMS) δ = 8.03−7.95 (2 H, m, Acenap 4,7-H), 7.54−7.48 (2 H, m, Acenap 3,8-H), 7.48−7.27 (10 H, m, Te$^+$*Ph* 12−16,19−23-H), 3.44 (4 H, s, 2 × CH_2), 3.02 (3 H, s, ^2J (H,Te) = 26.5, CH_3), 2.88 (3 H, s, ^2J (H,Te) = 26.7, CH_3). ^{125}Te NMR (81.2 MHz, CD_3CN, 25 °C, PhTeTePh): δ = 677(s). ^{19}F NMR (376.5 MHz, CD_3CN, 25 °C, CCl_3F): −79.84(s). MS (ES$^+$): *m*/*z* (%) 740.71 (95) [M$^+$ − OTf]. Anal. Calcd for $C_{28}H_{24}F_6O_6S_2Te_2$: C, 37.6; H, 2.7. Found: C, 37.6; H, 2.8.

Solid-State NMR Experimental Details. Solid-state NMR experiments were performed using a Bruker Avance III spectrometer operating at a magnetic field strength of 9.4 T. Experiments were carried out using a Bruker 4-mm probe at MAS rates of between 4 and 14 kHz (^{77}Se and ^{125}Te) and 12.5 kHz (^{13}C). ^{77}Se chemical shifts are referenced to $(CH_3)_2Se$ using the resonance of Na_2SeO_4 at 1058.7 ppm as a secondary reference. ^{125}Te chemical shifts are references relative to $(CH_3)_2Te$ using the resonance of $Te(OH)_6$ (site 1) at 692.2 ppm as a secondary reference. ^{13}C chemical shifts are referenced relative to tetramethylsilane using the CH_3 resonance of L-alanine at 20.5 ppm as a secondary reference. Transverse magnetization was obtained by cross-polarization from ^{1}H using optimized contact pulse durations of 10−15 ms (^{77}Se), 6−12 ms (^{125}Te), and 1−3 ms (^{13}C).

Two-pulse phase modulation ^{1}H decoupling was applied during acquisition. For compounds **A9-A13**, recycle intervals of 120 s were used. For compounds **9**−**13**, recycle intervals of 5 s were used.

Crystal Structure Analyses. X-ray crystal structures for **2**, **3**, **4**, **8**, **10**, and **13** were determined at −148(1) °C on the St Andrews Robotic Diffractometer[31] a Rigaku ACTOR-SM, Saturn 724 CCD area detector with graphite-monochromated Mo Kα radiation (λ = 0.71073 Å). Data was corrected for Lorentz, polarization, and absorption. Data for compounds **5**, **6**, and **11** were collected at −148(1) °C using a Rigaku MM007 high-brilliance RA generator (Mo Kα radiation, confocal optic) and Saturn CCD system. At least a full hemisphere of data was collected using ω scans. Intensities were corrected for Lorentz, polarization, and absorption. Data for compounds **7**, **9**, and **12** were collected at −148(1) °C on a Rigaku SCXmini CCD area detector with graphite-monochromated Mo Kα radiation (λ = 0.71073 Å). Data were corrected for Lorentz, polarization, and absorption. Data for **14** were collected at −180(1) °C using a Rigaku MM007 high-brilliance RA generator (Mo Kα radiation, confocal optic) and Mercury CCD system. At least a full hemisphere of data was collected using ω scans. Data for the complexes analyzed was collected and processed using CrystalClear (Rigaku).[32] Structures were solved by direct methods[33] and expanded using Fourier techniques.[34] Non-hydrogen atoms were refined anisotropically. Hydrogen atoms were refined using the riding model. All calculations were performed using the CrystalStructure[35] crystallographic software package except for refinement, which was performed using SHELXL-97.[36] These X-ray data can be obtained free of charge via www.ccdc.cam.ac.uk/conts/retrieving.html or from the Cambridge Crystallographic Data Centre, 12 Union Road, Cambridge CB2 1EZ, UK; fax (+44) 1223-336-033; e-mail: deposit@ccdc.cam.ac.uk.

Computational Details. Geometries were fully optimized in the gas phase at the B3LYP level[37] using Curtis and Binning's 962(d) basis[38] on Se, the Stuttgart−Dresden effective core potentials along with their double-ζ valence basis sets for Te[39] (augmented with d-polarization functions with exponents of 0.237),[40] and 6-31+G(d) basis elsewhere. Wiberg bond indices[41] and natural charges were obtained in a natural bond orbital analysis[42] at the same level. Optimizations were started from two different conformers for each compound **8**−**13**, labeled B-AA*t* and B-AA*c*. Experimental structures from X-ray crystallography were used as one of the starting conformers. Computations were performed using the Gaussian 03 suite of programs.[43] Selected relative energies were refined including the empirical dispersion corrections according to Grimme (denoted B3LYP-D3).[44]

■ ASSOCIATED CONTENT

Supporting Information

Full experimental details, solid-state NMR experimental details and interpretation, crystallographic data and figures, and computational details. This material is available free of charge via the Internet at http://pubs.acs.org.

■ AUTHOR INFORMATION

Corresponding Author

*E-mail: frk@st-andrews.ac.uk.

Notes

The authors declare no competing financial interest.

■ ACKNOWLEDGMENTS

Elemental analyses were performed by Stephen Boyer at the London Metropolitan University. Mass spectrometry was performed by Caroline Horsburgh. Calculations were performed using the EaStCHEM Research Computing Facility maintained by Dr. H. Früchtl. The work in this project was supported by the Engineering and Physical Sciences Research Council (EPSRC). M.B. wishes to thank EaStCHEM and the University of St. Andrews for support.

■ REFERENCES

(1) (a) Lewis, G. N. *Valence and the Structure of Atoms and Molecules*; The Chemical Catalog Co.: New York, 1923; Chapter 8. (b) Langmuir, I. *Science* **1921**, *54*, 59.

(2) Moss, G. P. *Pure Appl. Chem.* **1996**, *68*, 2193.

(3) (a) Bleiholder, C.; Werz, D. B.; Köppel, H.; Gleiter, R. *J. Am. Chem. Soc.* **2006**, *128*, 2666. (b) Steed, J. W.; Atwood, J. L. *Supramolecular Chemistry*; John Wiley & Sons: Chichester, 2000. (c) Schneider, H. J.; Yatsimirsky, A. *Principles and Methods in Supramolecular Chemistry*; John Wiley & Sons: Chichester, 2000.

(4) (a) Hatch, J. J.; Rundle, R. E. *J. Am. Chem. Soc.* **1951**, *73*, 4321. (b) Rundle, R. E. *J. Am. Chem. Soc.* **1963**, *85*, 112. (c) Rundle, R. E. *J. Am. Chem. Soc.* **1947**, *69*, 1327. (d) Sugden, S. *The Parachor and Valency*; Knopf: New York, 1930; Chapter 6. (e) Pimental, G. C. *J. Chem. Phys.* **1951**, *19*, 446. (f) In *The Nature of the Chemical Bond*, 3rd ed.; Pauling, L., Ed.; Cornell University Press, Ithaca, NY, 1960; Chapter 7. (g) Pauling, L. *J. Am. Chem. Soc.* **1947**, *69*, 542. (h) Coulson, C. A. d-Orbitals in Chemical Bonding. In *Proceedings of the Robert A. Welch Foundation Conferences on Chemical Research, XVI: Theoretical Chemistry*; Mulligen, W. O., Ed.; Robert A. Welch Foundation: Houston, TX, 1972; Chapter 3. (i) Brill, T. B. *J. Chem. Educ.* **1973**, *50*, 392. (j) Kutzelnigg, W. *Angew. Chem., Int. Ed.* **1984**, *23*, 272. (k) In *Valency and Bonding*; Weinhold, F., Landis, C., Eds.; Cambridge University Press: Cambridge, UK, 2005; Chapter 3.

(5) Bleiholder, C.; Gleiter, R.; Werz, D. B.; Köppel, H. *Inorg. Chem.* **2007**, *46*, 2249.

(6) (a) Pauling, L.; Corey, R. B.; Branson, H. R. *Proc. Natl. Acad. Sci. U.S.A.* **1951**, *37*, 205. (b) Pauling, L.; Corey, R. B. *Proc. Natl. Acad. Sci. U.S.A.* **1951**, *37*, 251. (c) Pauling, L.; Corey, R. B. *Proc. Natl. Acad. Sci. U.S.A.* **1951**, *37*, 729.

(7) (a) Desiraju, G. R.; Steiner, T. *The Weak Hydrogen Bond*; Oxford University Press: New York, 1999. (b) Steiner, T. *Angew. Chem., Int. Ed.* **2002**, *41*, 48. (c) Steiner, T. *Angew. Chem.* **2002**, *114*, 51.

(8) Nishio, M.; Hirota, M.; Umezawa, Y. *The CH/π-Interaction*; Wiley-VCH: New York, 1998.

(9) (a) Pedireddi, V. R.; Reddy, D. S.; Goud, B. S.; Craig, D. C.; Rae, A. D.; Desiraju, G. R. *J. Chem. Soc., Perkin Trans. 2* **1994**, 2353. (b) Rosenfield, R. E.; Parthasarathy, R.; Dunitz, J. D. *J. Am. Chem. Soc.* **1977**, *99*, 4860. (c) Guru Row, T. N.; Parthasarathy, R. *J. Am. Chem. Soc.* **1981**, *103*, 477. (d) Ramasubbu, N.; Parthasarathy, R. *Phosphorus Sulfur Silicon Relat. Elem.* **1987**, *31*, 221. (e) Glusker, J. P. *Top. Curr. Chem.* **1998**, *198*, 1. (f) Iwaoka, M.; Takemoto, S.; Okada, M.; Tomoda, S. *Bull. Chem. Soc. Jpn.* **2002**, *75*, 1611. (g) Corradi, E.; Meille, S. V.; Messina, M. T.; Metrangolo, P.; Resnati, G. *Angew. Chem., Int. Ed.* **2000**, *39*, 1782.

(10) For example, see: (a) Katz, H. E. *J. Am. Chem. Soc.* **1985**, *107*, 1420. (b) Alder, R. W.; Bowman, P. S.; Steel, W. R. S.; Winterman, D. R. *Chem. Commun.* **1968**, 723. (c) Costa, T.; Schimdbaur, H. *Chem. Ber.* **1982**, *115*, 1374. (d) Karacar, A.; Freytag, M.; Thönnessen, H.; Omelanczuk, J.; Jones, P. G.; Bartsch, R.; Schmutzler, R. *Heteroat. Chem.* **2001**, *12*, 102. (e) Glass, R. S.; Andruski, S. W.; Broeker, J. L.; Firouzabadi, H.; Steffen, L. K.; Wilson, G. S. *J. Am. Chem. Soc.* **1989**, *111*, 4036. (f) Fuji, T.; Kimura, T.; Furukawa, N. *Tetrahedron Lett.* **1995**, *36*, 1075. (g) Schiemenz, G. P. *Z. Anorg. All. Chem.* **2002**, *628*, 2597. (h) Corriu, R. J. P.; Young, J. C. In *Hypervalent Silicon Compounds, in Organic Silicon Compounds*; Patai, S., Rappoport, Z., Eds.; John Wiley & Sons Ltd.: Chichester, UK, 1989; Vols. *1* and *2*.

(11) (a) Nakanishi, W.; Hayashi, S.; Toyota, S. *Chem. Commun.* **1996**, 371. (b) Nakanishi, W.; Hayashi, S.; Sakaue, A.; Ono, G.; Kawada, Y. *J. Am. Chem. Soc.* **1998**, *120*, 3635. (c) Nakanishi, W.; Hayashi, S.; Toyota, S. *J. Org. Chem.* **1998**, *63*, 8790. (d) Hayashi, S.; Nakanishi, W. *J. Org. Chem.* **1999**, *64*, 6688. (e) Nakanishi, W.; Hayashi, S.; Uehara, T. *J. Phys. Chem. A* **1999**, *103*, 9906. (f) Nakanishi, W.; Hayashi, S.; Uehara, T. *Eur. J. Org. Chem.* **2001**, 3933. (g) Nakanishi, W.; Hayashi, S. *Phosphorus Sulfur Silicon Relat. Elem.* **2002**, *177*, 1833. (h) Nakanishi, W.; Hayashi, S.; Arai, T. *Chem. Commun.* **2002**, 2416. (i) Hayashi, S.; Nakanishi, W. *J. Org. Chem.* **2002**, *67*, 38. (j) Nakanishi, W.; Hayashi, S.; Itoh, N. *Chem. Commun.* **2003**, 124. (k) Hayashi, S.; Wada, H.; Ueno, T.; Nakanishi, W. *J. Org.*

Chem. **2006**, *71*, 5574. (l) Hayashi, S.; Nakanishi, W. *Bull. Chem. Soc. Jpn.* **2008**, *81*, 1605.
(12) (a) Coulson, C. A.; Daudel, R.; Robertson, J. M.; Proc., R. *Soc. London Ser. A.* **1951**, *207*, 306. (b) Cruickshank, D. W. *Acta Crystallogr.* **1957**, *10*, 504. (c) Brock, C. P.; Dunitz, J. D. *Acta Crystallogr., Sect. B* **1982**, *38*, 2218. (d) Oddershede, J.; Larsen, S. *J. Phys. Chem. A* **2004**, *108*, 1057.
(13) Hazell, A. C.; Hazell, R. G.; Norskov-Lauritsen, L.; Briant, C. E.; Jones, D. W. *Acta Crystallogr., Sect. C* **1986**, *42*, 690.
(14) (a) Aucott, S. M.; Milton, H. L.; Robertson, S. D.; Slawin, A. M. Z.; Walker, G. D.; Woollins, J. D. *Chem.—Eur. J.* **2004**, *10*, 1666. (b) Aucott, S. M.; Milton, H. L.; Robertson, S. D.; Slawin, A. M. Z.; Woollins, J. D. *Heteroat. Chem.* **2004**, *15*, 530. (c) Aucott, S. M.; Milton, H. L.; Robertson, S. D.; Slawin, A. M. Z.; Woollins, J. D. *Dalton Trans.* **2004**, 3347. (d) Aucott, S. M.; Kilian, P.; Milton, H. L.; Robertson, S. D.; Slawin, A. M. Z.; Woollins, J. D. *Inorg. Chem.* **2005**, *44*, 2710. (e) Aucott, S. M.; Kilian, P.; Robertson, S. D.; Slawin, A. M. Z.; Woollins, J. D. *Chem.—Eur. J.* **2006**, *12*, 895. (f) Aucott, S. M.; Duerden, D.; Li, Y.; Slawin, A. M. Z.; Woollins, J. D. *Chem.—Eur. J.* **2006**, *12*, 5495.
(15) (a) Kilian, P.; Slawin, A. M. Z.; Woollins, J. D. *Dalton Trans.* **2003**, 3876. (b) Kilian, P.; Slawin, A. M. Z.; Woollins, J. D. *Chem.—Eur. J.* **2003**, *9*, 215. (c) Kilian, P.; Slawin, A. M. Z.; Woollins, J. D. *Chem. Commun.* **2003**, 1174. (d) Kilian, P.; Milton, H. L.; Slawin, A. M. Z.; Woollins, J. D. *Inorg. Chem.* **2004**, *43*, 2252. (e) Kilian, P.; Slawin, A. M. Z.; Woollins, J. D. *Inorg. Chim. Acta* **2005**, *358*, 1719. (f) Kilian, P.; Slawin, A. M. Z.; Woollins, J. D. *Dalton Trans.* **2006**, 2175.
(16) (a) Knight, F. R.; Fuller, A. L.; Slawin, A. M. Z.; Woollins, J. D. *Dalton Trans.* **2009**, 8476. (b) Knight, F. R.; Fuller, A. L.; Slawin, A. M. Z.; Woollins, J. D. *Polyhedron* **2010**, *29*, 1849. (c) Knight, F. R.; Fuller, A. L.; Slawin, A. M. Z.; Woollins, J. D. *Polyhedron* **2010**, *29*, 1956. (d) Knight, F. R.; Fuller, A. L.; Slawin, A. M. Z.; Woollins, J. D. *Chem.—Eur. J.* **2010**, *16*, 7617.
(17) Knight, F. R.; Fuller, A. L.; Bühl, M.; Slawin, A. M. Z.; Woollins, J. D. *Chem.—Eur. J.* **2010**, *16*, 7503.
(18) (a) Knight, F. R.; Fuller, A. L.; Bühl, M.; Slawin, A. M. Z.; Woollins, J. D. *Inorg. Chem.* **2010**, *49*, 7577. (b) Knight, F. R.; Fuller, A. L.; Slawin, A. M. Z.; Woollins, J. D. *Eur. J. Inorg. Chem.* **2010**, 4034.
(19) Knight, F. R.; Fuller, A. L.; Bühl, M.; Slawin, A. M. Z.; Woollins, J. D. *Chem.—Eur. J.* **2010**, *16*, 7605.
(20) (a) Fuller, A. L.; Knight, F. R.; Slawin, A. M. Z.; Woollins, J. D. *Acta Crystallogr., Sect. E* **2007**, *E63*, o3855. (b) Fuller, A. L.; Knight, F. R.; Slawin, A. M. Z.; Woollins, J. D. *Acta Crystallogr., Sect. E* **2007**, *E63*, o3957. (c) Fuller, A. L.; Knight, F. R.; Slawin, A. M. Z.; Woollins, J. D. *Acta Crystallogr., Sect. E* **2008**, *E64*, o977.
(21) Aschenbach, L. K.; Knight, F. R.; Randall, R. A. M.; Cordes, D. B.; Baggott, A.; Bühl, M.; Slawin, A. M. Z.; Woollins, J. D. *Dalton Trans.* **2012**, *41*, 3141.
(22) Knight, F. R.; Athukorala Arachchige, K. S.; Randall, R. A. M.; Bühl, M.; Slawin, A. M. Z.; Woollins, J. D. *Dalton Trans.* **2012**, *41*, 3154.
(23) Fujihara, H.; Ishitani, H.; Takaguchi, Y.; Furukawa, N. *Chem. Lett.* **1995**, *24*, 571.
(24) Balzer, G.; Duddeck, H.; Fleischer, U.; Röhr, F. *Fresenius' J. Anal. Chem.* **1997**, *357*, 473.
(25) Griffin, J. M.; Knight, F. R.; Hua, G.; Ferrara, J. S.; Hogan, S. W. L.; Woollins, J. D.; Ashbrook, S. E. *J. Phys. Chem. C* **2011**, *115*, 10859.
(26) Nagy, P.; Szabó, D.; Kapovits, I.; Kucsman, Á.; Argay, G.; Kálmán, A. *J. Mol. Struct.* **2002**, *606*, 61.
(27) Bondi, A. *J. Phys. Chem.* **1964**, *68*, 441.
(28) For example, for the parent 1,8-bis(dimethylphosphine) naphthalene, see: Jones, P. G.; Thonnessen, H.; Karacar, A.; Schmutzler, R. *Acta Crystallogr., Sect. C* **1997**, *53*, 1119.
(29) Wiberg, K. B. *Tetrahedron* **1968**, *24*, 1083.
(30) Reed, A. E.; Curtiss, F.; Weinhold, L. A. F. *Chem. Rev.* **1988**, *88*, 899.
(31) Fuller, A. L.; Scott-Hayward, L. A. S.; Li, Y.; Bühl, M.; Slawin, A. M. Z.; Woollins, J. D. *J. Am. Chem. Soc.* **2010**, *132*, 5799.
(32) *CrystalClear 1.6*; Rigaku Corp.: The Woodlands, TX, 1999. *CrystalClear Software User's Guide*; Molecular Structure Corp.: The Woodlands, TX, 2000. Flugrath, J. W. P. *Acta Crystallogr., Sect. D* **1999**, *D55*, 1718.
(33) SIR97: Altomare, A.; Burla, M.; Camalli, M.; Cascarano, G.; Giacovazzo, C.; Guagliardi, A.; Moliterni, A.; Polidori, G.; Spagna, R. *J. Appl. Crystallogr.* **1999**, *32*, 115.
(34) DIRDIF99: Beurskens, P. T.; Admiraal, G.; Beurskens, G.; Bosman, W. P.; de Gelder, R.; Israel, R.; Smits, J. M. M. The DIRDIF-99 program system. *Technical Report of the Crystallography Laboratory*; University of Nijmegen: The Netherlands, 1999.
(35) *CrystalStructure 3.8.1: Crystal Structure Analysis Package*; Rigaku and Rigaku/MSC: The Woodlands, TX, 2000–2006.
(36) SHELX97: Sheldrick, G. M. *Acta Crystallogr., Sect. A* **2008**, *64*, 112.
(37) (a) Becke, A. D. *J. Chem. Phys.* **1993**, *98*, 5648. (b) Lee, C.; Yang, W.; Parr, R. G. *Phys. Rev. B* **1988**, *37*, 785.
(38) Binning, R. C.; Curtiss, L. A. *J. Comput. Chem.* **1990**, *11*, 1206.
(39) (a) Schwerdtfeger, P.; Dolg, M.; Schwarz, W. H. E.; Bowmaker, G. A.; Boyd, P. D. W. *J. Chem. Phys.* **1989**, *91*, 1762. (b) Bergner, A.; Dolg, M.; Kuechle, W.; Stoll, H.; Preuss, H. *Mol. Phys.* **1993**, *80*, 1431. (c) For I the valence basis by Kaupp et al. (including diffuse functions) was employed: Kaupp, M.; Schleyer, P. v. R.; Stoll, H.; Preuss, H. *J. Am. Chem. Soc.* **1991**, *113*, 6012.
(40) Huzinaga, S.; Anzelm, J.; Klobukowski, M.; Radzio-Andzelm, E.; Sakai, Y.; Tatewaki, H. In *Gaussian Basis Sets for Molecular Calculations*; Elsevier: Amsterdam, 1984.
(41) Wiberg, K. B. *Tetrahedron* **1968**, *24*, 1083.
(42) Reed, A. E.; Curtiss, F.; Weinhold, L. A. F. *Chem. Rev.* **1988**, *88*, 899.
(43) Pople, J. A.; et al. *Gaussian 03*, Revision E.01; Gaussian, Inc.: Wallingford, CT, 2004 (for a full citation see ref S8, Supporting Information).
(44) Grimme, S.; Antony, J.; Ehrlich, S.; Krieg, H. *J. Chem. Phys.* **2010**, *132*, 154104.